JGP Journal of General Physiology

ARTICLE

Excitation–Contraction Coupling

Specific ATPases drive compartmentalized glycogen utilization in rat skeletal muscle

Joachim Nielsen[1], Peter Dubillot[1], Marie-Louise H. Stausholm[1], and Niels Ørtenblad[1]

Glycogen is a key energy substrate in excitable tissue, including in skeletal muscle fibers where it also contributes to local energy production. Transmission electron microscopy imaging has revealed the existence of a heterogenic subcellular distribution of three distinct glycogen pools in skeletal muscle, which are thought to reflect the requirements for local energy stores at the subcellular level. Here, we show that the three main energy-consuming ATPases in skeletal muscles (Ca^{2+}, Na^+,K^+, and myosin ATPases) utilize different local pools of glycogen. These results clearly demonstrate compartmentalized glycogen metabolism and emphasize that spatially distinct pools of glycogen particles act as energy substrate for separated energy requiring processes, suggesting a new model for understanding glycogen metabolism in working muscles, muscle fatigue, and metabolic disorders. These observations suggest that the distinct glycogen pools can regulate the functional state of mammalian muscle cells and have important implications for the understanding of how the balance between ATP utilization and ATP production is regulated at the cellular level in general and in skeletal muscle fibers in particular.

Introduction

It is of vital importance for all cell types to balance energy utilization and production, but it is particularly important in excitable cells with high fluctuations in energy turnover. A close match between energy utilization and production is established by functional compartmentalization of enzymatic reactions (Welch, 1977; Saks et al., 2008), which ensures rapid exchange of metabolites. In skeletal muscle, this has probably evolved because of multiple constraints as cell size, spatial distribution of energy consuming and producing processes, and a physical constraint imposed by intracellular structures limiting free diffusion (Srere, 1967). Still, within this organization, glycogen particles are distributed in local depositions and thereby serve as an efficient energy store for the different steps in excitation–contraction (E-C) coupling and relaxation. Intriguingly, glycogen particles and glycogenolytic and glycolytic enzymes are observed adjacent to the sarcoplasmic reticulum (SR) membrane (Garant, 1968; Wanson and Drochmans, 1968), and it is well described how this physical association directs a crosstalk, where Ca^{2+} release from the SR upon muscle activation facilitates glycogen degradation and glycolytic ATP production and, reversely, where glycogen loss impairs SR function (Tammineni et al., 2020; Ørtenblad et al., 2011). The glycogen–glycogenolytic–glycolytic system is an example of functional compartmentalization, where the specific organization and localization of enzymes and glycogen particles create an efficient delivery of energy to energy requiring processes located in specific subcellular domains (Lynch and Paul, 1983; Dhar-Chowdhury et al., 2007). Thus, the diffusional barrier by intracellular structures is circumvented by situating the metabolic machinery and the glycogen particles close to the energy consuming processes, where one pool of glycogen particles may preferentially serve the neighboring ATPases.

In working skeletal muscle fibers, myosin ATPases, SR Ca^{2+} ATPases, and Na^+,K^+ ATPases consume ∼50–60%, 40–50%, and 5–10% of the energy, respectively, depending on contraction mode (Ørtenblad et al., 2009; Clausen et al., 1991). In order to clarify whether these three major energy consuming processes utilize different pools of glycogen particles, we conducted two main sets of experiments, where we stimulated or inhibited specific energy consumption by the different ATPases combined with measures of the distinct pools of glycogen particles by quantitative transmission electron microscopy (TEM).

[1]Department of Sports Science and Clinical Biomechanics, University of Southern Denmark, Odense, Denmark.

Correspondence to Joachim Nielsen: jnielsen@health.sdu.dk

This work is part of a special issue on excitation–contraction coupling.

Materials and methods

Animals

All handling and use of animals complied with Danish animal welfare regulations. Experiments were performed using 4–6-wk-old male Wistar rats of own breed, weighing 102–276 g, which were kept in a thermostated environment at 21°C with a 12/12 h light-dark cycle and fed ad libitum at the Biomedical Laboratory, University of Southern Denmark.

Experimental design

Myosin ATPase inhibition

Soleus muscles of Sprague Dawley rats (4–6-wk-old males weighing 112–276 g, killed by cervical dislocation) were mounted to a force transducer and bathed in a standard Krebs-Ringer bicarbonate buffer at 30°C continuously gassed with a mixture of 95% O_2 and 5% CO_2. After 30 min of rest in the standard KR buffer, the muscles were incubated for 180 min with either 50 µM N-benzyl-p-toluene sulfonamide (BTS; Cheung et al., 2002) and 25 µM blebbistatin (Straight et al., 2003) or vehicle (DMSO; 0.3% volume). Then, muscles were either tetanic stimulated (30 Hz for 400 ms every 2 s) or rested for 20 min.

Na^+,K^+-ATPase inhibition

Soleus muscles of Sprague Dawley rats (4–6-wk-old males weighing 102–192 g, killed by cervical dislocation) were mounted to a force transducer and bathed in a standard Krebs-Ringer bicarbonate buffer and 1 mM ouabain or vehicle (water) at 30°C continuously gassed with a mixture of 95% O_2 and 5% CO_2. After 30 min of rest, the muscles were incubated for 60 min with either 10 µM salbutamol or vehicle (methanol; 2% volume).

Force measurements

Muscles were mounted for isometric contractions in thermostated chambers containing standard Krebs-Ringer bicarbonate buffer and adjusted to optimal length for force production. Force was measured using force transducers and recorded with a chart recorder and digitally on a computer.

Krebs-Ringer solution for in vitro incubation of soleus muscles

All in vitro experiments were performed with muscles incubated in a standard Krebs-Ringer bicarbonate buffer containing the following (in mM): 122.1 NaCl, 25.1 $NaCHO_3$, 2.8 KCl, 1.2 KH_2PO_4, 1.2 $MgSO_4$, 1.3 $CaCl_2$, and 5.0 D-glucose (pH 7.4). All chemicals were of analytical grade and unless stated were obtained from Sigma-Aldrich, with BTS obtained from Toronto Research Chemicals, Ontario, Canada.

Determination of muscle glycogen and lactate concentration

Homogenate glycogen concentration was determined by spectrophotometry (Beckman DU 650) in a glucose-NADPH coupled assay according to Lowry and Passonneau (1972). Freeze-dried muscle tissue (1.5 mg) was boiled in 0.5 ml 1 M HCL for 150 min before it was rapidly cooled, whirl-mixed, and centrifuged at 3,500 *g* for 10 min at 4°C. 40 µl of boiled muscle sample and 1 ml of reagent solution containing Tris-buffer (1 M), distilled water, ATP (100 mM), $MgCl_2$ (1 M), $NADP^+$ (100 mM), and G-6-PDH were mixed before the process was initiated by adding 10 µl of diluted hexokinase and absorbance was recorded for 60 min and expressed as mmol glycosyl units per kg dry weight (dw). Lactate was determined from specimen, which was freeze-dried, dissected free of nonmuscle tissue, powdered and extracted with $HClO_4$. Lactate was expressed as mmol·kg^{-1} dw.

Quantitative TEM

Preparation of samples for glycogen staining

Muscle samples were prepared for analyses of the subcellular distribution of glycogen as previously described in detail (Jensen et al., 2022). Briefly, a small piece (<1 mm^3) of the mid-belly of m. soleus was fixed in 2.5% glutaraldehyde in 0.1 M sodium cacodylate buffer (pH 7.3) for 24 h at 4°C and subsequently rinsed four times in 0.1 M sodium cacodylate buffer. Following rinsing, the muscle pieces were postfixed with 1% osmium tetroxide (OsO_4) and 1.5% potassium ferrocyanide ($K_4Fe(CN)_6$) in 0.1 M sodium cacodylate buffer for 90 min at 4°C. The use of potassium ferrocyanide during post fixation enhances the visualization of glycogen particles. After postfixation, the muscle pieces were rinsed twice in 0.1 M sodium cacodylate buffer for 60 min at 4°C, dehydrated through a graded series of alcohol at 4–20°C, infiltrated with graded mixtures of propylene oxide and Epon at 20°C, and embedded in 100% Epon at 30°C. Ultra-thin (60 nm) sections were cut (using a Leica Ultracut UCT ultramicrotome) in two depths (separated by 150 µm) and contrasted with uranyl acetate and lead citrate. Sections were examined and three longitudinal oriented fibers per muscle were photographed in a precalibrated TEM (JEM-1400Plus; JEOL Ltd. and a Quemesa camera). Images were analyzed by a blinded investigator using a digital screen at a final total magnification of 100,000×.

Quantification of the subcellular distribution of glycogen

The volume fraction of glycogen in three distinct localizations was estimated using standard stereological techniques (Weibel, 1980). Since glycogen particles (diameter of 10–40 nm) are smaller than the thickness of the section (60 nm), the calculation of the volume fraction based on an area fraction on the projected images is corrected for an overestimation due to a cutting by the upper and lower slice surface and thereby abrogating the spherical shape of some of the particles. This is done by the formula suggested by Weibel (1980): $V_V = A_A - t\{(1/\pi)\cdot B_A - N_A\cdot[(t \times H)/(t + H)]\}$, where A_A is glycogen area fraction, t is the section thickness (60 nm), B_A is the glycogen boundary length density (i.e., the perimeter of the glycogen particle profiles per area of muscle region), N_A is the number of particles per area ($A_A/(\pi \times \frac{1}{2}H^2)$), and H is the average glycogen particle diameter. Glycogen particles were assumed to be spherical. A_A was estimated by point counting using different grid sizes for the different locations in order to achieve satisfactorily precision of the estimates (see below). B_A was calculated as $\pi/4 \times S_V + t \times N_V \times \pi \times H$, where S_V is $N_V \times \pi \times H^2$ and N_V is $N_A/(t + H)$.

The average glycogen particle diameter for each location was calculated by directly measuring at least 60 particles per location per fiber using iTEM (iTEM software, version 5.0; Olympus). However, of the 284 fibers analyzed, only 40–59 particles could be found in 72 fibers and only 10–39 particles in 24 fibers.

Intermyofibrillar glycogen was expressed relative to the myofibrillar space and estimated using grid sizes of 120 and 300 nm, respectively. The amount of intramyofibrillar glycogen was expressed relative to the intramyofibrillar space and estimated using grid sizes of 60 and 300 nm, respectively. The subsarcolemmal glycogen was expressed relative to the muscle fiber surface area and estimated using a grid size of 90 nm. The fiber surface area was estimated by measuring directly the length of the fiber accompanying with the area of the subsarcolemmal region, which is perpendicular to the outer most myofibril and then multiplied by the section thickness (60 nm).

Statistics

Results are shown as means and SD, geometric means, and 95% confidence interval, or box plots displaying the first and third quartiles and split by the median with *n* representing the number of fibers included from the number of rats. The normality of data distribution was determined by Q–Q plots and the constant variance across groups by plotting the predicted values against the residuals. If necessary, data were transformed as indicated in the figure legends. Linear mixed effect model was used to investigate interaction and main effects. $P < 0.05$ was considered to be statistically significant. The exact statistical parameters are indicated in the figure legends. No data was excluded for statistical analysis. Statistical analyses were done in Stata/IC 16 (StataCorp). Investigators were blinded to allocation during image analyses.

Results

Three subcellular pools of glycogen were defined based on their spatial distribution (Fig. 1, A–C). To embrace fiber-to-fiber variation, we estimated the volumetric content at the single fiber level, where coefficient of errors between 0.15 and 0.25 could be obtained after analyses of 12–16 images per fiber (Fig. 1 D). The TEM estimated total glycogen volume fraction correlated well with biochemically determined mixed glycogen concentration from homogenates (Fig. 1 E). In the resting control muscles combined from both experiments, glycogen particles were distributed with 65, 29, and 6% as intermyofibrillar, intramyofibrillar, and subsarcolemmal glycogen, respectively (Fig. 1 F).

Myosin ATPase inhibition

In the first experiment, the myosin ATPase was selectively inhibited while normal E–C coupling was maintained (Macdonald et al., 2005), enabling the estimation of the magnitude of location specific glycogen consumption associated with both myosin ATPase and SR Ca^{2+} ATPase activity. Selective inhibition of the myosin ATPase activity by BTS and blebbistatin nearly abolished the tetanic stimulation-induced force production (Fig. 2 A), which, as expected, was accompanied by a marked lowered utilization of mixed muscle glycogen (Fig. 2 B) accompanied by less accumulation of lactate (Fig. 2 C) after the stimulation protocol.

In resting muscles, the volumetric content of intermyofibrillar glycogen was unaffected by myosin ATPase inhibition ($P = 0.69$; Fig. 2 D). Electrical stimulation mediated a ∼40% ($P < 0.001$) decrease in control muscles, which was attenuated to a ∼30% ($P = 0.004$) decrease in muscles with myosin ATPase inhibition (two-way interaction: $P = 0.008$; Fig 2, D and E).

The volumetric content of intramyofibrillar glycogen was also unaffected or decreased slightly by myosin ATPase inhibition in resting muscles ($P = 0.06$; Fig. 2 F). While electrical stimulation mediated a ∼90% ($P < 0.001$) reduction in intramyofibrillar glycogen of control muscles, the myosin ATPase inhibition completely abolished this stimulation-mediated reduction in intramyofibrillar glycogen ($P = 0.67$; two-way interaction: $P = 0.008$; Fig. 2, F and G)

Subsarcolemmal glycogen content (Fig. 2, H and I) was not affected by electrical stimulation (main effect, $P = 0.22$), myosin ATPase inhibition (main effect, $P = 0.58$), nor both combined (two-way interaction, $P = 0.40$).

Na^+,K^+-ATPase inhibition

To investigate if Na^+,K^+-ATPase activity is connected to the utilization of a local pool of glycogen, muscles were exposed to the β-adrenoceptor agonist salbutamol, which stimulate the Na^+,K^+ ATPase (Clausen and Overgaard, 2000), combined with the cardiac glycoside ouabain, which selectively block the Na^+,K^+ ATPase (Lingrel and Kuntzweiler, 1994). Here, salbutamol mediated a reduction in mixed glycogen concentration and an increase in lactate concentration, which was attenuated by ouabain (Fig. 3, H and I).

Ouabain mediated a small ∼10% increase in intermyofibrillar glycogen (main effect of ouabain: $P = 0.001$) but did not affect a ∼40% reduction in intermyofibrillar glycogen by salbutamol exposure (main effect of salbutamol: $P < 0.001$; ouabain-salbutamol interaction: $P = 0.16$; Fig. 3, A and B).

While ouabain alone did not affect intramyofibrillar glycogen levels ($P = 0.49$), it attenuated a salbutamol-induced reduction in intramyofibrillar glycogen (ouabain-salbutamol interaction: $P = 0.01$; Fig. 3, C and D). At the single fiber level, this could be explained by an effect of ouabain on the lower quartile value, where salbutamol alone decreased the lower quartile value by ∼66%, which was attenuated to a decrease of ∼25% in ouabain treated muscles.

No or only small effects of salbutamol (main effect, $P = 0.25$), ouabain (main effect, $P = 0.84$), or both combined (two-way interaction, $P = 0.64$) were found for subsarcolemmal glycogen (Fig. 3, E and F).

Discussion

Here, we show that selectively inhibition of myosin ATPase activity during electrical stimulation and inhibition of Na^+,K^+ ATPase activity during β-adrenoceptor stimulation affect the subcellular utilization of glycogen in skeletal muscle fibers. This is demonstrated in rat soleus muscle consisting of mainly type 1 fibers and suggests that the myosin ATPases equally utilize glycogen from both the intra- and intermyofibrillar compartments, the SR Ca^{2+} ATPases utilize glycogen only from the intermyofibrillar compartment, and the Na^+,K^+ ATPases utilize glycogen only from the intramyofibrillar compartment.

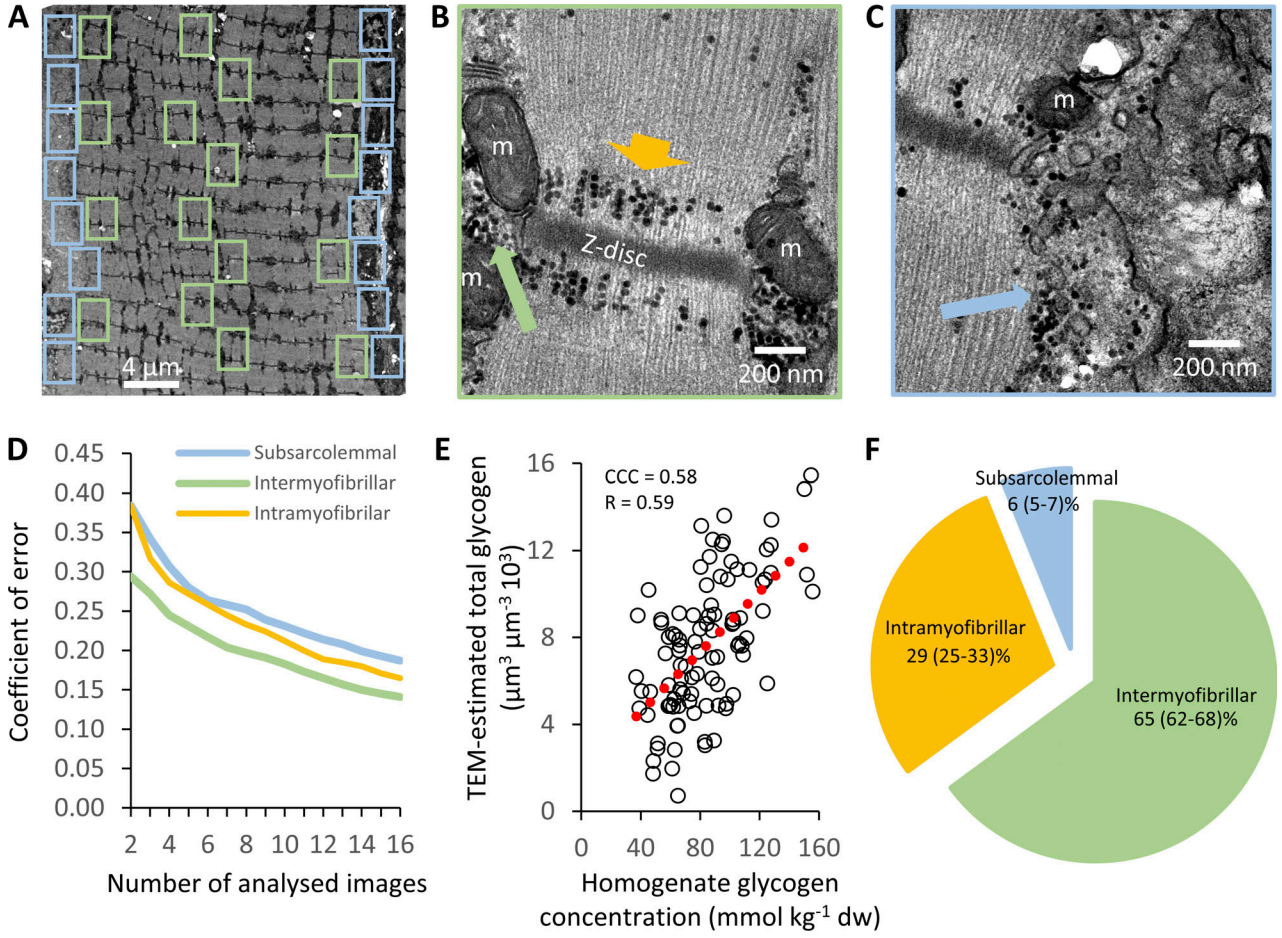

Figure 1. **TEM analyses of subcellular glycogen distribution. (A)** Fixed muscle segments were prepared for glycogen visualization by TEM and cut in longitudinal sections. Three fibers were photographed per muscle in a randomized systematic order including 12–16 images from the subsarcolemmal region and 12–16 images from the myofibrillar region. **(B)** In the myofibrillar images, the volumetric content of intermyofibrillar glycogen (long green arrow) and intramyofibrillar glycogen (short orange arrow) was estimated by point counting (Nielsen et al., 2011; Weibel, 1980). **(C)** In the subsarcolemmal images, the volume of subsarcolemmal glycogen (blue arrow) per fiber surface area was estimated by point counting and a fiber length measurement (Jensen et al., 2022). **(D)** After completion of analysis of the first 102 fibers, image-to-image variation showed a mean stereological coefficient of error of 0.14, 0.17, and 0.19 after analysis of 16 images for intermyofibrillar, intramyofibrillar, and subsarcolemmal glycogen, respectively. It was decided for the remaining fibers (n = 172) that 12 photographed images were sufficient per region. **(E)** Scatterplot of TEM-estimated total glycogen per muscle (mean of three fibers) versus the glycogen concentration determined from a homogenate. Concordance correlation coefficient (CCC) showed a moderate agreement between the two methods. R indicates Person's correlation coefficient. Dotted red line indicates best linear fit. **(F)** The relative distribution (in percent) of the three pools to the total volumetric content. Values are mean and 95% confidence interval. n = 60 fibers from 20 rats.

It is well described that the activity of the three main ATPases is connected to glycogen metabolism. The SR Ca^{2+} ATPase and Na^+,K^+ ATPase seem to be directly fueled by glycolysis as shown by studies using inhibitors of glycolysis and glycogenolysis (Glitsch and Tappe, 1993; Xu et al., 1995; Kockskämper et al., 2005; Jensen et al., 2020). The activity of the myosin ATPase is to a large extent supported by the creatine kinase reaction breaking down PCr (Chung et al., 1998), which is then resynthesized by glycogen breakdown and glycolysis (Shulman et al., 2001). Such functional compartmentalization may exist due to the physical association of glycolytic enzymes at the SR membrane (Entman et al., 1980), the t-tubular membrane (Han et al., 1992), and the actin filaments within the myofibrils (Arnold and Pette, 1968). In line with this compartmentalized organization of the cell, we demonstrate that the three muscle cell glycogen pools are selectively used by the ATPases.

Here, we show that a possible profound role of glycogen to support the energetics of contractility (i.e., myosin ATPase activity) results in a very high depletion of intramyofibrillar glycogen. Since it is reasoned that only glycogen breakdown can produce the ATP at the necessary high rate (Shulman et al., 2001), it is intriguingly that the absolute amount of intramyofibrillar glycogen in skeletal muscle fibers seems well conserved across different species despite large differences in the other pools of glycogen (Nielsen et al., 2014 and this study). Thus, in resting muscles, most fibers store around 3–8 μm^3 μm^{-3} 10^3 (Nielsen et al., 2011). A depletion of intramyofibrillar glycogen during muscle work to levels <2 μm^3 μm^{-3} 10^3 has been linked to muscle fatigue as described by lower tetanic free Ca^{2+} concentrations (Nielsen et al., 2014) and SR Ca^{2+} release rate (Ørtenblad et al., 2011). However, low intramyofibrillar glycogen is not always associated with depressed SR Ca^{2+} release rate

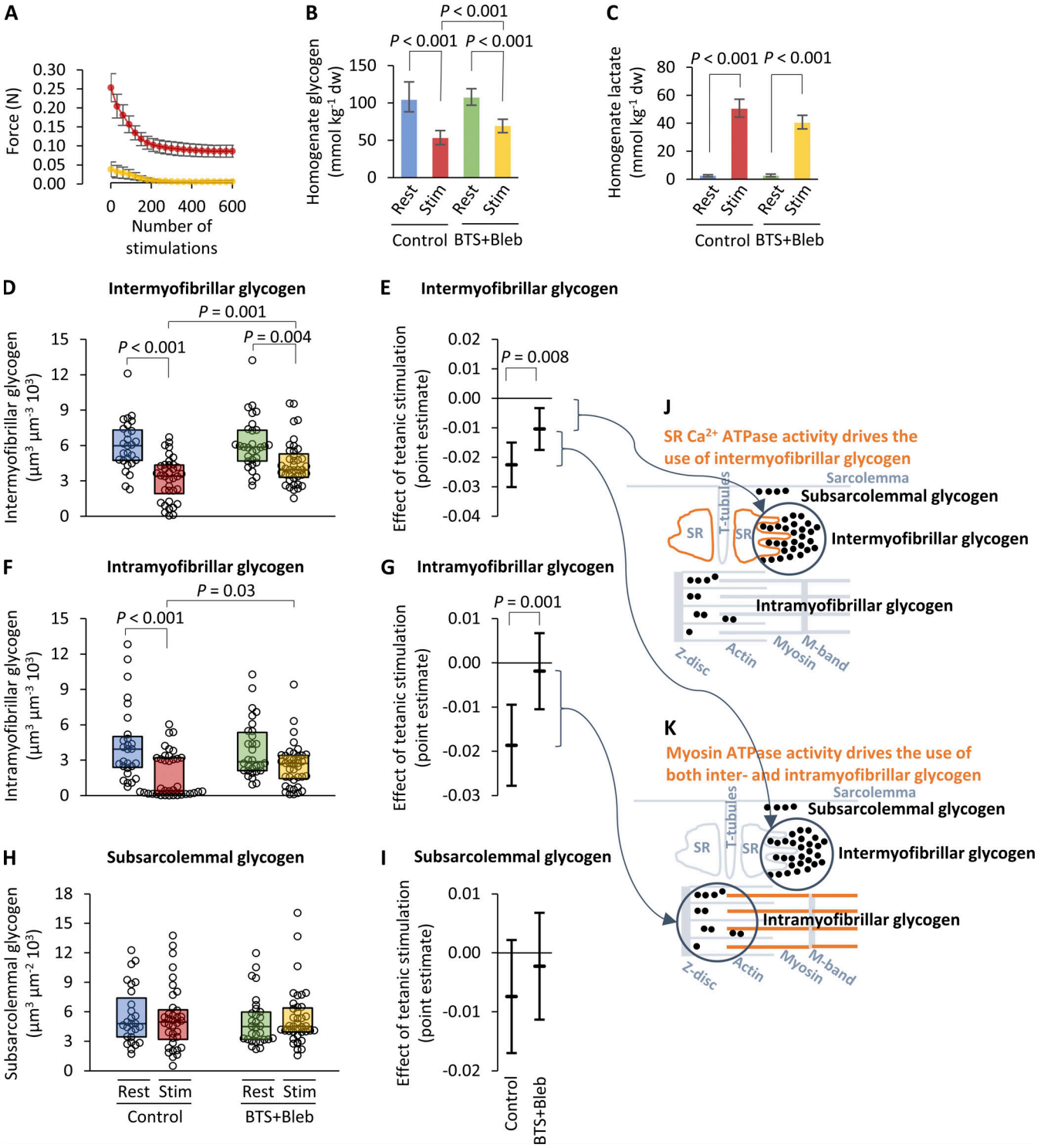

Figure 2. **Effect of myosin ATPase inhibition during tetanic stimulation on subcellular compartmentalized glycogen metabolism. (A)** Force production during repeated tetanic stimulations in control muscles (red) and in muscles with the myosin ATPase inhibited (BTS + Bleb; yellow) shown as mean and SD. *n* = 12–13 muscles. **(B)** Muscle homogenate glycogen concentration shown as mean with 95% confidence interval. *n* = 9–13 rats. **(C)** Muscle homogenate lactate concentration shown as geometric mean with 95% confidence interval. *n* = 9–13 rats. **(D, F, and H)** Single-fiber values of glycogen in three distinct subcellular pools: intermyofibrillar, intramyofibrillar, and subsarcolemmal. Data are shown as box plots displaying the first and third quartiles and split by the median. *n* = 27–39 fibers from 9 to 13 muscles. **(E, G, and I)** Point estimates with 95% confidence interval from linear mixed effect model on square root-transformed data from D. **(J and K)** Illustrations of the spatial association between SR Ca^{2+} ATPases situated at the SR membrane (orange in F) and intermyofibrillar glycogen, and between the myosin ATPases (orange in G) and inter- and intramyofibrillar glycogen. Interaction or main effects were tested using linear mixed-effect model on square root–transformed data with tetanic stimulation and myosin ATPase inhibitors as fixed effects and rat ID as random effect. P values for two-way interactions were 0.008, 0.001, 0.395, 0.039, and 0.045 for intermyofibrillar, intramyofibrillar, subsarcolemmal glycogen, homogenate glycogen, and homogenate lactate, respectively.

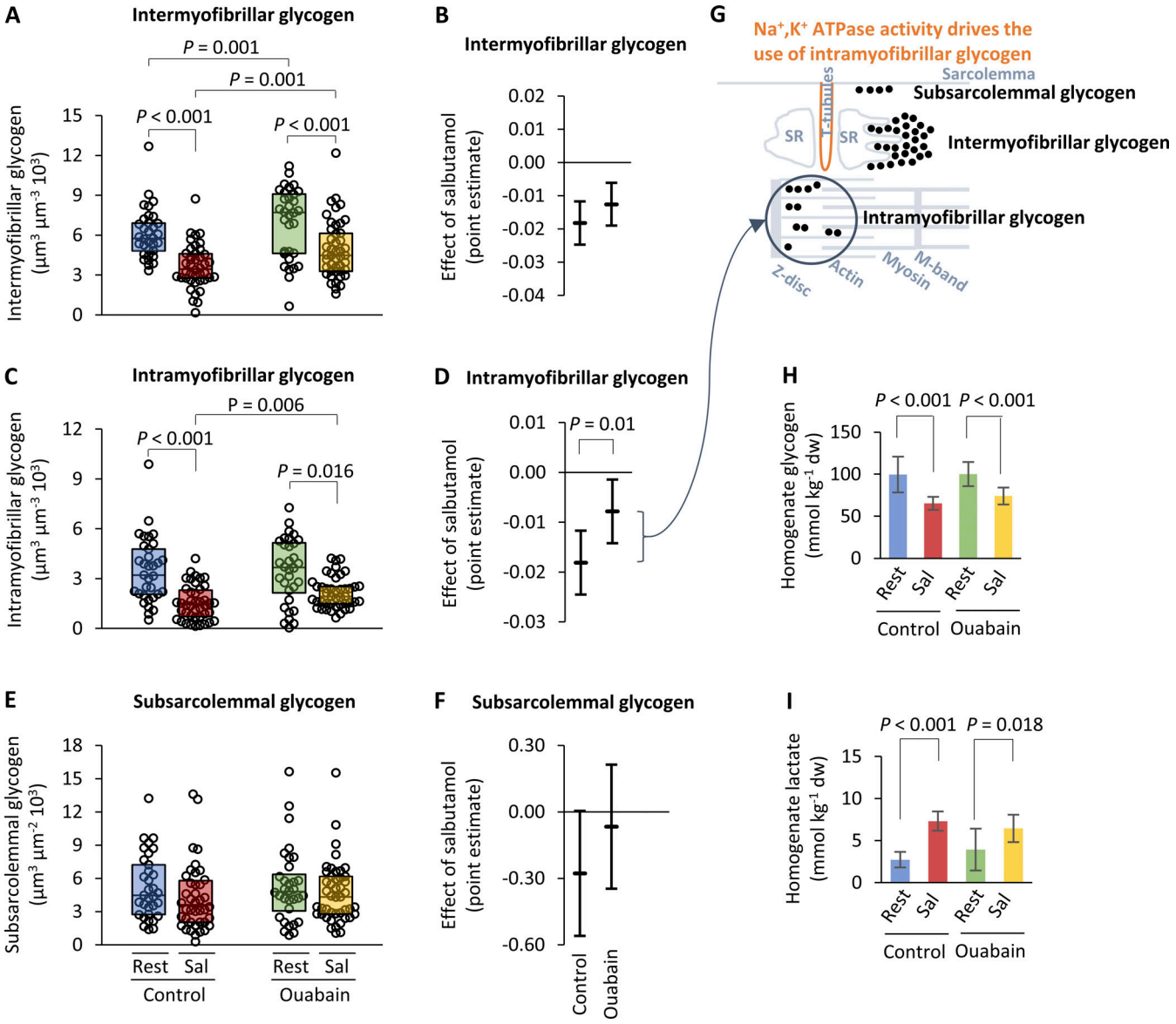

Figure 3. **Effect of Na⁺,K⁺-ATPase inhibition during salbutamol exposure on subcellular compartmentalized glycogen metabolism. (A, C, and E)** Single-fiber values of glycogen in three distinct subcellular pools: intermyofibrillar, intramyofibrillar, and subsarcolemmal. Data are shown as box plots displaying the first and third quartiles and split by the median. *n* = 32–45 fibers from 11 to 16 muscles. **(B, D, and F)** Point estimates with 95% confidence interval from linear mixed effect model on square root–transformed data from (intermyofibrillar and intramyofibrillar glycogen) or log-transformed data (subsarcolemmal glycogen) from A. **(G)** Illustrations of the spatial association between Na⁺,K⁺ ATPases situated at the t-tubular membrane (orange) and intramyofibrillar glycogen. **(H)** Muscle homogenate glycogen concentration shown as mean with 95% confidence interval. *n* = 11–16 muscles. **(I)** Muscle homogenate lactate concentration shown as mean with 95% confidence interval. *n* = 11–16 muscles. Interaction or main effects were tested using linear mixed effect model on square root–transformed (intermyofibrillar and intramyofibrillar glycogen in A and C, respectively), log-transformed (subsarcolemmal glycogen in E), or nontransformed data (H and I) with salbutamol and ouabain as fixed effects and rat as random effect. P values for two-way interactions were 0.164, 0.010, 0.225, 0.281, and 0.052 for intermyofibrillar, intramyofibrillar, subsarcolemmal glycogen, homogenate glycogen, and homogenate lactate, respectively.

(Krustrup et al., 2011; Nielsen et al., 2012). The latter study assessed glycogen content and SR Ca^{2+} release rate after a soccer match and only during recovery (with no pre-exercise biopsy). It could be that the muscle damage associated with the soccer match (Krustrup et al., 2011) has masked any relationship between glycogen and SR Ca^{2+} release rate. Nevertheless, multiple linear regression analyses have shown that intramyofibrillar glycogen impacts endurance capacity more than the two other pools of glycogen in humans (Jensen et al., 2020b). It remains to be investigated whether low intramyofibrillar glycogen affects PCr resynthesis, myosin ATPase activity, and contractility. We observed a high variability in intramyofibrillar glycogen content from fiber to fiber of the present study. Some of this variability may originate from our definition the subcellular pools of glycogen, where all glycogen particles localized within the myofibrils are defined as intramyofibrillar glycogen. This could be a too simple definition since exercise may mediate a larger utilization of I-band glycogen than of A-band glycogen (Fridén et al.,

1989). It is therefore reasonable that some of the heterogeneity in single fiber glycogen originates from our man-made definitions of subcellular glycogen pools and, hence, that another approach involving automated pattern recognition could provide valuable additional information.

Since intermyofibrillar glycogen constitutes the largest fraction of total glycogen, the effect of myosin ATPase inhibition on stimulation-induced changes in intermyofibrillar glycogen resembles the changes in homogenate mixed muscle glycogen. By blocking the myosin ATPase, the utilization of intramyofibrillar glycogen was almost completely abolished, while the utilization of intermyofibrillar glycogen was reduced by about 25–50% (Fig. 2, D and E). Since the intermyofibrillar pool contains twice the amount of glycogen than the intramyofibrillar pool, the myosin ATPase taxes those two pools approximately equally in absolute quantity. When the myosin ATPase is blocked, the SR Ca^{2+} ATPase represents the majority (>80%) of the remaining energy consumption during contractions, of which the requirement for glycogen therefore can be exclusively connected to the utilization of intermyofibrillar glycogen. An important experimental limitation of the present design is that the muscles are expected to have been partly anoxic during the electrical stimulation protocol due to limitations in oxygen diffusion during the present contractile duty cycle (Barclay, 2005). Therefore, the findings may not be extrapolated to muscles working with adequate O_2 levels, where mitochondrial oxidative phosphorylation to a larger extent can contribute to the ATP production. In line with this limitation, the present observation that the myosin ATPase equally utilizes glycogen from both the intra- and intermyofibrillar compartments may not be uniformly valid for all contraction modalities or duty cycles. The myosin ATP turnover is generally accepted to accounts for 50–80% of the ATP consumed during most muscle contractions of maximal or near maximal force (Kushmerick, 1988; Walsh et al., 2006; Barclay et al., 2008; Ørtenblad et al., 2009), suggesting little effects of changing contractile duty cycle on relative ATP turnover by the different ATPases.

This differential glycogen utilization by the myosin ATPases and SR Ca^{2+} ATPases is in line with the idea of a functional compartmentalization of energy production and utilization in the muscle cell and the proximity of the pools and the specific ATPases (Fig. 2, J and K). In support, we have found in mechanically skinned fibers, where global ATP and PCr can be kept high and constant, that the rate of force decay after a tetanic contraction correlated with intermyofibrillar glycogen. This suggests that this specific pool of glycogen may provide energy for the SR Ca^{2+} ATPase and, in turn, relaxation of force (Nielsen et al., 2009). It is noteworthy that during tetanic stimulation with blocked myosin ATPases the Na^+,K^+ ATPases are also stimulated and could therefore also be a utilizer of glycogen. However, they represent <20% of the energy turnover and it is therefore not possible to make valid interpretations of their connection to the utilization of local pools of glycogen in this specific condition. Therefore, we explored in a second experiment if their activity is linked to a local pool of glycogen using resting muscles based on an experimental design with β-adrenoceptor stimulation (James et al., 1999).

In this second experiment with inhibition of the Na^+,K^+-ATPase activity during β-adrenoceptor stimulation, we found that Na^+,K^+-ATPase activity may only use intramyofibrillar glycogen. These data are in line with a study using similar experimental design and determination of glycogen in a mixed muscle homogenate (James et al., 1999). While SR Ca^{2+} ATPases and myosin ATPases are closely associated with glycogen particles, the Na^+,K^+-ATPase activity occurs in the t-tubular system and the sarcolemma, which is not colocalized with intramyofibrillar glycogen (Fig. 3 C). However, glycolytic enzymes are abundant in the t-tubular membrane (Han et al., 1992), bound to the actin filaments within the sarcomeres (Arnold and Pette, 1968) and to the glycogen particles (Meyer et al., 1970), creating the structural basis for a functional compartmentalization with distant glycogen particles. This functional compartmentalization can exist through sequential steps in the glycolytic pathway creating a channeling mechanism (Ovádi and Srere, 2000). Interestingly, a disruption of this spatial organization of glycolytic enzymes in *Drosophila melanogaster* flight muscle leads to an inability of the flies to fly (Wojtas et a. 1997).

A possible connection between intramyofibrillar glycogen and processes occurring in the triadic gap between the SR and the t-tubular system is supported by our previous findings showing an association between intramyofibrillar glycogen and both excitability (Nielsen et al., 2009) and SR Ca^{2+} release rate (Ørtenblad et al., 2011). Interestingly, the effect of ouabain on the salbutamol-induced glycogen reduction was most pronounced in the fibers with the lower quartile glycogen content, suggesting that some fibers were more sensitive to ouabain than others and/or that part of the salbutamol-induced glycogen reduction could not be attenuated by ouabain. Regarding the former a potential variability in ouabain sensitivity could be related to the fibers' proportion of specific α-subunits, which have large differences in their affinity for ouabain (O'Brien et al., 1994). Regarding the latter, salbutamol may induce Ca^{2+} leak from the SR (Cairns and Borrani, 2015), which in turn, will increase SR Ca^{2+} ATPase activity (Meizoso-Huesca et al., 2022). However, a possible Ca^{2+} leak may only affect intermyofibrillar glycogen but can then explain why the salbutamol-induced reduction in intermyofibrillar glycogen is not attenuated with ouabain.

We observed a clear effect of ouabain on the salbutamol-induced utilization of intramyofibrillar glycogen, but no or only a small effect on the utilization of subsarcolemmal glycogen. This differential effect may be due to an uneven distribution of α subunits between the t-system and sarcolemmal with α1 subunit exclusively present at the sarcolemmal and α2 subunit present in both the sarcolemma and t-system (Radzyukevich et al., 2013) combined with a higher sensitivity of α2 subunit for ouabain (O'Brien et al., 1994) and maybe also salbutamol. Another explanation could be the broad definition of subsarcolemmal glycogen as all glycogen particles localized between the sarcolemma and the outermost myofibril. This broad definition could comprise several independent subpools of subsarcolemmal glycogen as peri-nuclei, peri-mitochondrial, and sarcolemmal-bound, where only the sarcolemmal-bound subpool may be related to the Na^+,K^+-ATPase activity.

In the present experiment, we showed a link between Na^+,K^+-ATPase activity and intramyofibrillar glycogen in rested

muscles. Noteworthy, this should be confirmed in active muscles with action potential–activated Na^+,K^+ ATPases, with a much higher overall energy turnover, and with a potential concomitant competition between ATPases for specific glycogen pools. The present investigation was limited to the assessment of glycogen stores which prevent any calculations of substrate partitioning. Thus, glucose uptake and catabolism could have contributed with production of ATP.

In conclusion, the three main energy-consuming processes in working skeletal muscle fibers, the myosin ATPase, the SR Ca^{2+} ATPase, and the Na^+,K^+ ATPase, are connected to the utilization of spatially distinct pools of glycogen in the soleus muscle of rats. We suggest that a competition between the myosin ATPases and the Na^+,K^+ ATPases for intramyofibrillar glycogen creates a link, where contractility is connected to excitability. This explains why muscles devoid of glycogen due to a prior sustained high consumption rate or inherited diseases suffer from muscle fatigue (Chin and Allen, 1997) and exercise intolerance (De Stafano et al., 1996). These results further suggest a mechanism whereby the muscle fiber with low glycogen can restrain the energy turnover by inhibiting SR Ca^{2+} turnover and membrane excitability. This would decrease the muscle fiber ATP utilization and keep a vital balance between energy utilization and production.

Acknowledgments

Eduardo Ríos served as editor.

The experiments were performed at the Department of Sports Science and Clinical Biomechanics (in vitro experiments and metabolite analyses) and Institute of Pathology, Faculty of Health Science (TEM analyses), University of Southern Denmark, DK-5230 M, Denmark. We thank Kirsten Hansen and Karin Trampedach for skillful technical assistance.

This study was supported by a grant from the Ministry of Culture Committee on Sports Research (TKIF2011-058).

The authors declare no competing financial interests.

Author contributions: J. Nielsen contributed with conceptualization, formal analysis, investigation, data curation, writing—original draft, visualization, supervision, project administration, and funding acquisition. P. Dubillot contributed with conceptualization, formal analysis, investigation, writing—review and editing, and visualization. M.-L.H. Stausholm contributed with investigation and writing—review and editing. N. Ørtenblad contributed with conceptualization, investigation, writing—review and editing, and supervision.

Submitted: 31 January 2022
Accepted: 22 June 2022

References

Arnold, H., and D. Pette. 1968. Binding of glycolytic enzymes to structure proteins of the muscle. *Eur. J. Biochem.* 6:163–171. https://doi.org/10.1111/j.1432-1033.1968.tb00434.x

Barclay, C.J. 2005. Modelling diffusive O_2 supply to isolated preparations of mammalian skeletal and cardiac muscle. *J. Muscle Res. Cell Motil.* 26: 225–235. https://doi.org/10.1007/s10974-005-9013-x

Barclay, C.J., G.A. Lichtwark, and N.A. Curtin. 2008. The energetic cost of activation in mouse fast-twitch muscle is the same whether measures using reduced filament overlap or *N*-benzyl-*p*-toluenesulphonamide. *Acta Physiol.* 193:381–391. https://doi.org/10.1111/j.1748-1716.2008.01855.x

Cairns, S.P., and F. Borrani. 2015. β-Adrenergic modulation of skeletal muscle contraction: Key role of excitation-contraction coupling. *J. Physiol.* 593: 4713–4727. https://doi.org/10.1113/JP270909

Cheung, A., J.A. Dantzig, S. Hollingworth, S.M. Baylor, Y.E. Goldman, T.J. Mitchison, and A.F. Straight. 2002. A small-molecule inhibitor of skeletal muscle myosin II. *Nat. Cell Biol.* 4:83–88. https://doi.org/10.1038/ncb734

Chin, E.R., and D.G. Allen. 1997. Effects of reduced muscle glycogen concentration on force, Ca^{2+} release and contractile protein function in intact mouse skeletal muscle. *J. Physiol.* 498 (Pt 1):17–29. https://doi.org/10.1113/jphysiol.1997.sp021838

Chung, Y., R. Sharman, R. Carlsen, S.W. Unger, D. Larson, and T. Jue. 1998. Metabolic fluctuation during a muscle contraction cycle. *Am. J. Physiol.* 274:C846-52. https://doi.org/10.1152/ajpcell.1998.274.3.C846

Clausen, T., and K. Overgaard. 2000. The role of K^+ channels in the force recovery elicited by Na-K-pump stimulation in Ba^{2+}-paralysed rat skeletal muscle. *J. Physiol.* 527 Pt 2:325–332. https://doi.org/10.1111/j.1469-7793.2000.00325.x

Clausen, T., C. Van Hardeveld, and M.E. Everts. 1991. Significance of cation transport in control of energy metabolism and thermogenesis. *Physiol. Rev.* 71:733–774. https://doi.org/10.1152/physrev.1991.71.3.733

De Stefano, N., Z. Argov, P.M. Matthews, G. Karpati, and D.L. Arnold. 1996. Impairment of muscle mitochondrial oxidative metabolism in McArdles's disease. *Muscle Nerve.* 19:764–769. https://doi.org/10.1002/(SICI)1097-4598(199606)19:6<764::AID-MUS12>3.0.CO;2-L

Dhar-Chowdhury, P., B. Malester, P. Rajacic, and W.A. Coetzee. 2007. The regulation of ion channels and transporters by glycolytically derived ATP. *Cell. Mol. Life Sci.* 64:3069–3083. https://doi.org/10.1007/s00018-007-7332-3

Entman, M.L., S.S. Keslensky, A. Chu, and W.B. Van Winkle. 1980. The sarcoplasmic reticulum-glycogenolytic complex in mammalian fast twitch skeletal muscle. Proposed in vitro counterpart of the contraction-activated glycogenolytic pool. *J. Biol. Chem.* 255:6245–6252.

Fridén, J., J. Seger, and B. Ekblom. 1989. Topographical localization of muscle glycogen: An ultrahistochemical study in the human vastus lateralis. *Acta Physiol. Scand.* 135:381–391. https://doi.org/10.1111/j.1748-1716.1989.tb08591.x

Garant, P.R. 1968. Glycogen-membrane complexes within mouse striated muscle cells. *J. Cell Biol.* 36:648–652. https://doi.org/10.1083/jcb.36.3.648

Glitsch, H.G., and A. Tappe. 1993. The Na+/K+ pump of cardiac Purkinje cells is preferentially fuelled by glycolytic ATP production. *Pflugers Arch.* 422: 380–385. https://doi.org/10.1007/BF00374294

Han, J.-W., R. Thieleczek, M. Varsanyi, and L.M.G. Heilmeyer Jr. 1992. Compartmentalized ATP synthesis in skeletal muscle triads. *Biochemistry.* 31:377–384. https://doi.org/10.1021/bi00117a010

James, J.H., K.R. Wagner, J.-K. King, R.E. Leffler, R.K. Upputuri, A. Balasubramanian, L.A. Friend, D.A. Shelly, R.J. Paul, and J.E. Fischer. 1999. Stimulation of both aerobic glycolysis and Na+-K+-ATPase activity in skeletal muscle by epinephrine or amylin. *Am. J. Physiol.* 277:E176–E186. https://doi.org/10.1152/ajpendo.1999.277.1.E176

Jensen, R., J. Nielsen, and N. Ørtenblad. 2020. Inhibition of glycogenolysis prolongs action potential repriming period and impairs muscle function in rat skeletal muscle. *J. Physiol.* 598:789–803. https://doi.org/10.1113/JP278543

Jensen, R., N. Ørtenblad, M.H. Stausholm, M.C. Skjaerbaek, D.N. Larsen, M. Hansen, H.C. Holmberg, P. Plomgaard, and J. Nielsen. 2020b. Heterogeneity in subcellular muscle glycogen utilisation during exercise impacts endurance capacity in men. *J. Physiol.* 598:4271–4292. https://doi.org/10.1113/JP280247

Jensen, R., N. Ørtenblad, C. di Benedetto, K. Qvortrup, and J. Nielsen. 2022. Quantification of subcellular glycogen distribution in skeletal muscle fibers using transmission electron microscopy. *JoVE.* https://doi.org/10.3791/63347

Kockskämper, J., A.V. Zima, and L.A. Blatter. 2005. Modulation of sarcoplasmic reticulum Ca2+ release by glycolysis in cat atrial myocytes. *J. Physiol.* 564:697–714. https://doi.org/10.1113/jphysiol.2004.078782

Krustrup, P., N. Ortenblad, J. Nielsen, L. Nybo, T.P. Gunnarsson, F.M. Iaia, K. Madsen, F. Stephens, P. Greenhaff, and J. Bangsbo. 2011. Maximal voluntary contraction force, SR function and glycogen resynthesis during

the first 72 h after a high-level competitive soccer game. *Eur. J. Appl. Physiol.* 111:2987–2995. https://doi.org/10.1007/s00421-011-1919-y

Kushmerick, M.J. 1988. Energetics of muscle contraction. *In Handbook of Physiology. Skeletal Muscle.* L.D. Peachey, editor. American Physiological Society, Bethesda, MD. 189–236.

Lingrel, J., and T. Kuntzweiler. 1994. Na+, K+-ATPase. *J. Biol. Chem.* 269: 19659–19662. https://doi.org/10.1016/s0021-9258(17)32067-7

Lowry, O.H., and J.V. Passonneau. 1972. A Flexible System on Enzymatic Analysis. Academic Press, New York.

Lynch, R.M., and R.J. Paul. 1983. Compartmentation of glycolytic and glycogenolytic metabolism in vascular smooth muscle. *Science*. 222: 1344–1346. https://doi.org/10.1126/science.6658455

Macdonald, W.A., T.H. Pedersen, T. Clausen, and O.B. Nielsen. 2005. N-Benzyl-p-toluene sulphonamide allows the recording of trains of intracellular action potentials from nerve-stimulated intact fast-twitch skeletal muscle of the rat. *Exp. Physiol.* 90:815–825. https://doi.org/10.1113/expphysiol.2005.031435

Meizoso-Huesca, A., L. Pearce, C.J. Barclay, and B.S. Launikonis. 2022. Ca^{2+} leak through ryanodine receptor 1 regulates thermogenesis in resting skeletal muscle. *Proc. Natl. Acad. Sci. USA*. 119:e2119203119. https://doi.org/10.1073/pnas.2119203119

Meyer, F., L.M. Heilmeyer Jr., R.H. Haschke, and E.H. Fischer. 1970. Control of phosphorylase activity in a muscle glycogen particle. I. Isolation and characterization of the protein-glycogen complex. *J. Biol. Chem.* 245: 6642–6648. https://doi.org/10.1016/s0021-9258(18)62582-7

Nielsen, J., A.J. Cheng, N. Ørtenblad, and H. Westerblad. 2014. Subcellular distribution of glycogen and decreased tetanic Ca^{2+} in fatigued single intact mouse muscle fibres. *J. Physiol.* 592:2003–2012. https://doi.org/10.1113/jphysiol.2014.271528

Nielsen, J., H.C. Holmberg, H.D. Schrøder, B. Saltin, and N. Ørtenblad. 2011. Human skeletal muscle glycogen utilization in exhaustive exercise: Role of subcellular localization and fibre type. *J. Physiol.* 589:2871–2885. https://doi.org/10.1113/jphysiol.2010.204487

Nielsen, J., P. Krustrup, L. Nybo, T.P. Gunnarsson, K. Madsen, H.D. Schrøder, J. Bangsbo, and N. Ortenblad. 2012. Skeletal muscle glycogen content and particle size of distinct subcellular localizations in the recovery period after a high-level soccer match. *Eur. J. Appl. Physiol.* 112: 3559–3567. https://doi.org/10.1007/s00421-012-2341-9

Nielsen, J., H.D. Schrøder, C.G. Rix, and N. Ørtenblad. 2009. Distinct effects of subcellular glycogen localization on tetanic relaxation time and endurance in mechanically skinned rat skeletal muscle fibres. *J. Physiol.* 587:3679–3690. https://doi.org/10.1113/jphysiol.2009.174862

O'Brien, W.J., J.B. Lingrel, and E.T. Wallick. 1994. Ouabain binding kinetics of the rat alpha two and alpha three isoforms of the sodium-potassium adenosine triphosphate. *Arch. Biochem. Biophys.* 310:32–39. https://doi.org/10.1006/abbi.1994.1136

Ovádi, J., and P.A. Srere. 2000. Macromolecular compartmentation and channeling. *Int. Rev. Cytol.* 192:255–280. https://doi.org/10.1016/s0074-7696(08)60529-x

Ørtenblad, N., W.A. Macdonald, and K. Sahlin. 2009. Glycolysis in contracting rat skeletal muscle is controlled by factors related to energy state. *Biochem. J.* 420:161–168. https://doi.org/10.1042/BJ20082135

Ørtenblad, N., J. Nielsen, B. Saltin, and H.C. Holmberg. 2011. Role of glycogen availability on SR Ca^{2+} kinetics in human skeletal muscle. *J. Physiol.* 589: 711–725. https://doi.org/10.1113/jphysiol.2010.195982

Radzyukevich, T.L., J.C. Neumann, T.N. Rindler, N. Oshiro, D.J. Goldhamer, J.B. Lingrel, and J.A. Heiny. 2013. Tissue-specific role of the Na, K-ATPase α2 isozyme in skeletal muscle. *J. Biol. Chem.* 288:1226–1237. https://doi.org/10.1074/jbc.M112.424663

Saks, V., N. Beraud, and T. Wallimann. 2008. Metabolic compartmentation: A system level property of muscle cells: Real problems of diffusion in living cells. *Int. J. Mol. Sci.* 9:751–767. https://doi.org/10.3390/ijms9050751

Shulman, R.G., F. Hyder, and D.L. Rothman. 2001. Cerebral energetics and the glycogen shunt: Neurochemical basis of functional imaging. *Proc. Natl. Acad. Sci. USA*. 98:6417–6422. https://doi.org/10.1073/pnas.101129298

Srere, P.A. 1967. Enzyme concentrations in tissues. *Science*. 158:936–937. https://doi.org/10.1126/science.158.3803.936

Straight, A.F., A. Cheung, J. Limouze, I. Chen, N.J. Westwood, J.R. Sellers, and T.J. Mitchison. 2003. Dissecting temporal and spatial control of cytokinesis with a myosin II inhibitor. *Science*. 299:1743–1747. https://doi.org/10.1126/science.1081412

Tammineni, E.R., N. Kraeva, L. Figueroa, C. Manno, C.A. Ibarra, A. Klip, S. Riazi, and E. Rios. 2020. Intracellular calcium leak lowers glucose storage in human muscle, promoting hyperglycemia and diabetes. *eLife*. 9:e53999. https://doi.org/10.7554/eLife.53999

Walsh, B., R.A. Howlett, C.M. Stary, C.A. Kinding, and M.C. Hogan. 2006. Measurement of activation energy and oxidative phosphorylation onset kinetics in isolated muscle fibers in the absence of cross-bridge cycling. *Am. J. Physiol. Regul. Integr. Comp. Physiol.* 290:R1707–R1713. https://doi.org/10.1152/ajpregu.00687.2005

Wanson, J.C., and P. Drochmans. 1968. Rabbit skeletal muscle glycogen. A morphological and biochemical study of glycogen beta-particles isolated by the precipitation-centrifugation method. *J. Cell Biol.* 38:130–150. https://doi.org/10.1083/jcb.38.1.130

Weibel, E.R. 1980. Stereological Methods. Vol. 2. Theoretical Foundations. Academic Press, London.

Welch, G.R. 1977. On the role of organized multienzyme systems in cellular metabolism: A general synthesis. *Prog. Biophys. Mol. Biol.* 32:103–191. https://doi.org/10.1016/b978-0-08-020295-2.50006-4

Wojtas, K., N. Slepecky, L. von Kalm, and D. Sullivan. 1997. Flight muscle function in Drosophila requires colocalization of glycolytic enzymes. *Mol. Biol. Cell*. 8:1665–1675. https://doi.org/10.1091/mbc.8.9.1665

Xu, K.Y., J.L. Zweier, and L.C. Becker. 1995. Functional coupling between glycolysis and sarcoplasmic reticulum Ca2+ transport. *Circ. Res.* 77: 88–97. https://doi.org/10.1161/01.res.77.1.88